Point sur la situation du projet Super-Kamiokande et sur l'engagement des équipes IN2P3

L. Bernard[1], A. Coffani[1], O. Drapier[1], S. El-Hedri[1], A. Giampaolo[1], M. Gonin[2], Th. A. Mueller[1], P. Paganini[1], B. Quilain[1], and A. Santos[1]

[1]Laboratoire Leprince-Ringuet
[2]International Research Laboratory ILANCE

September 24, 2021

The Laboratoire Leprince-Ringuet (LLR) joined the Super-Kamiokande (SK) collaboration in 2017. Presently, the group is composed of 9 members as shown in Table 1. In spring 2021, Michel Gonin (DRCE) has left our group to take the head of the IRL ILANCE which has just been created. ILANCE has therefore also joined the collaboration. For the LLR, our funding from IN2P3 is of approximately 5 k€ per physicist per year and was 40 k€ in 2021. This budget is mainly used for collaboration meetings and shifts in Japan. We have received 140 k€ from Ecole polytechnique in 2018 which have been used for the major refurbishment work (both on-site work & material purchases). We can also count on the European funding program H2020 (SK2HK [1]) which can help us paying our travel expenses to Japan.

Name	Position	FTE
Laura BERNARD	Post-doc	1
Alice COFFANI	PhD student	1
Olivier DRAPIER	DR1	0.2
Sonia EL-HEDRI	Post-doc	1
Alberto GIAMPAOLO	PhD student	1
Thomas MUELLER	CRCN	0.4
Pascal PAGANINI	DR1	0.8
Benjamin QUILAIN	CRCN	0.1
Andrew SANTOS	PhD tracks	N/A

Table 1: Current composition of the LLR Super-Kamiokande group.

1 The Super-Kamiokande experiment

Super-Kamiokande is a 50 kton water Cherenkov detector located beneath a one-km rock overburden (2.7 km water-equivalent) within the Kamioka mine in Japan. The SK detector, shown schematically in figure 1, consists of two concentric, optically separated, water Cherenkov detectors contained in a cylindrical steel tank with a diameter of 39.3 m and a height of 42 m. The inner detector (ID) has a diameter of a 33.8 m and a height of 36.2 m which in the end represents a fiducial mass of 22.5 kiloton. Its surface is equipped with 11146 inward-facing large photomultiplier tubes (PMTs) for a coverage of 40%. The surface of the outer detector (OD) is instrumented with 1885 PMTs with a diameter of 20 cm.

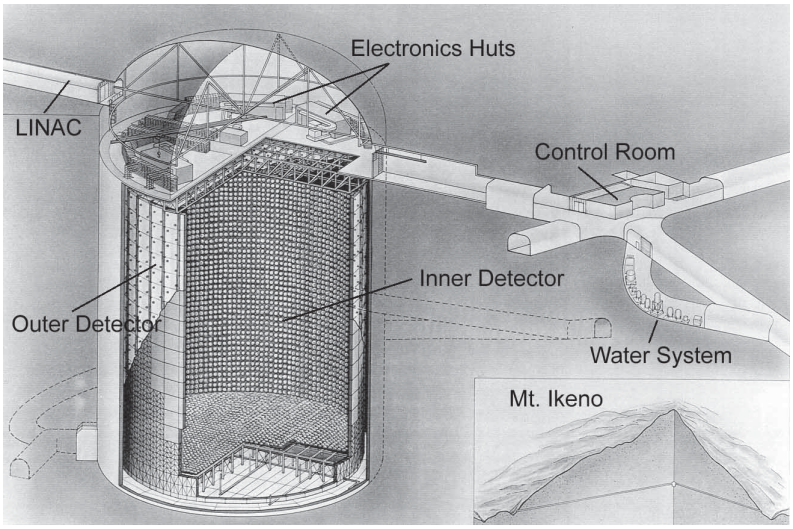

Figure 1: The Super-Kamiokande detector [2].

The SK experiment has collected data during 6 different phases summarized in Table 2. Current analyses use the data for the first four phases (from SK-I to SK-IV). This corresponds to a combined exposure of 372.6 kton.years. Details of detector design, performance, calibration, data reduction and simulations can be found in [2, 3]. In 2018, a major refurbishment of the detector was accomplished in order to add Gadolinium (Gd) to increase the sensitivity of SK to detect neutrons. This work included, among others, water sealing reinforcement, improvement of tank piping, and replacement of defective PMTs. Each IN2P3 member of the SK collaboration at that time spent 2 weeks on site between June and September 2018 to perform this work.

Phase	Period	Event
SK-I	1996 to 2001	Start of the experiment
SK-II	2003 to 2005	20% photo-coverage after accident
SK-III	2006 to 2008	Full photo-coverage (40%) restored
SK-IV	2008 to 2018	Upgraded electronics
SK-V	2019 to 2020	Detector upgraded for Gd-loading
SK-VI	since 2020	0.01% Gd-doping

Table 2: Summary of the different phases of the Super-Kamiokande experiment.

SK is a highly versatile multi-purpose experiment, with capability to explore variety of topics in the MeV - TeV energy range. This includes, among others, physics related to solar and atmospheric neutrinos, supernovae neutrinos, diffuse supernovae neutrino background (DSNB), neutrino astrophysics, and the study of dark matter as well as proton decay and other baryon number-violating processes. The SK detector also serves as far detector for T2K [4] which is a long baseline neutrino oscillation experiment. This experiment, in which many members of IN2P3 are involved, is presented in a separate document [5].

In this report, we will present the status and perspectives for the physics analysis of atmospheric neutrinos oscillations as requested by the scientific council of IN2P3, and for the search for the DSNB, as it represents the major contribution of our group to the physics analysis at SK.

2 Status of the experiment

2.1 Atmospheric neutrinos oscillations

Atmospheric neutrinos is the named given to neutrinos produced by the interaction of primary cosmic rays (mostly protons) with the nuclei in the Earth's atmosphere. These interactions lead to the production of mesons which will subsequently decay into neutrinos through for example

$$\pi^+ \to \mu^+ + \nu_\mu, \quad \mu^+ \to e^+ + \nu_e + \bar{\nu}_\mu \tag{1}$$

as well as their antiparticle counterpart. Atmospheric neutrinos therefore represent a permanent isotropic flux of ν_μ, $\bar{\nu}_\mu$, ν_e and $\bar{\nu}_e$ with energies ranging from about 100 MeV to 100 GeV. Collecting atmospheric neutrinos from all directions, SK can probe a wide range of about $10 - 10^4$ km propagation baselines. From the multiplicities of neutrinos in the process (1) it is clear that at low energies ($E \leq 1$ GeV), for which most muons decay before hitting the ground, the neutrino flux satisfies

$$\frac{\phi_{\nu_\mu} + \phi_{\bar{\nu}_\mu}}{\phi_{\nu_e} + \phi_{\bar{\nu}_e}} \simeq 2. \tag{2}$$

At energies higher than 1 GeV the fraction of muons hitting the ground before decaying increases, leading to an increase of the flavour ratio. Atmospheric neutrino interactions in the SK detector are simulated using the flux calculations of Honda *et al.* [6] and the NEUT [7] neutrino interaction software. Detector simulations based on GEANT-3 track particles resulting from the interactions.

Depending on the topology and on the ID and OD activities, SK atmospheric data is divided into fully contained (FC), partially contained (PC) and upward-going muon (UPμ) events. FC events have their vertices reconstructed within the fiducial volume but almost no OD activity, PC events have OD activity corresponding to exiting particles, and UPμ events are from muon neutrinos interacting with the rock below the detector and depositing energy in both OD and ID. Those samples are further categorized according to various characteristics such as the number of decay electrons and Cherenkov rings, their energies, and whether the rings are showering (e-like) or non-showering (μ-like). SK's excellent particle identification capabilities (PID, see Fig. 2 for example) allows for a clear flavour separation. The $\nu/\bar{\nu}$ separation can only be done statistically for multi-ring events, since ν events tend to have more rings than $\bar{\nu}$ events. In SK-IV, neutron tagging through capture on hydrogen has become feasible (25% efficiency), allowing separation into $\nu/\bar{\nu}$ for single ring events.

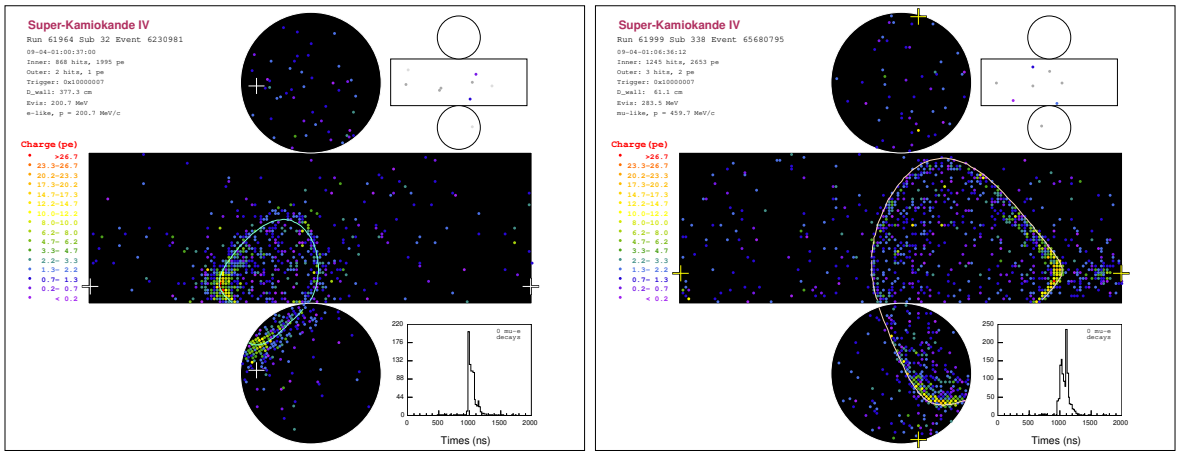

Figure 2: Typical e-like (left) and mu-like (right) event display in SK. The mis-PID probability at ~ 1 GeV is of about 2%.

Oscillation parameters can be measured by studying either the disappearance of $\nu_\mu/\bar{\nu}_\mu$ and the appearance of $\nu_e/\bar{\nu}_e$. It is through the model-independent observation of a deficit of atmo-

spheric upward-going vs. downward going ν_μ that SK discovered neutrino oscillation in 1998 [8]. No such effect has been seen for ν_e implying that ν_μ mostly oscillate into ν_τ. Subsequently, SK has detected the appearance of ν_τ [9].

Neutrinos propagating through the Earth experience matter effects due to the modification of the Hamiltonian stemming from the difference in forward coherent scattering of ν_e and $\nu_{\mu,\tau}$. This is characterized via

$$H_{\text{eff}} = \frac{1}{2E} U_{\text{PMNS}} \mathbb{M}^2 U_{\text{PMNS}}^\dagger + \text{diag}(V_e, 0, 0), \qquad \mathbb{M}^2 = \begin{pmatrix} 0 & 0 & 0 \\ 0 & \Delta m^2_{21} & 0 \\ 0 & 0 & \Delta m^2_{31} \end{pmatrix} \tag{3}$$

where $V_e = \sqrt{2} G_F N_e$, G_F being the Fermi constant and N_e the electron number density. For anti-neutrinos, V_e changes sign. Matter resonance effects in neutrino oscillations occur only for neutrinos if the hierarchy is normal (NH, $\Delta m^2_{32} > 0$) and only for anti-neutrinos if it is inverted (IH, $\Delta m^2_{32} < 0$). Those effects are depicted on the oscillograms of Fig. 3 are more pronounced either for upward-going multi-GeV ν_e or for $\bar{\nu}_e$, thus giving sensitivity to the mass hierarchy.

The atmospheric oscillation analysis is based on a simultaneous fit to θ_{23}, Δm^2_{32} and δ_{CP} for each hierarchy assumption. The value of θ_{13} is constrained to $\sin^2\theta_{13} = 0.0218$ as measured by reactor experiments [11][1]. The fit results for the full SK-I to IV are shown on Fig. 4 and Tab. 3. The data prefers θ_{23} to be in the 1$^{\text{st}}$ octant and favors NH at 1.7σ level ($\Delta\chi^2(\text{IH}) - \Delta\chi^2(\text{NH}) = 2.8$) as well as $\delta_{\text{CP}} \sim 3\pi/2$ consistent with the T2K results [12]. For the unconstrained fit, the value of θ_{13} is consistent with reactor and long baseline experiments. The atmospheric mixing parameters are displayed on Fig. 5 for the NH and compared to most recent results from other experiments.

930 bins	χ^2	$\sin^2\theta_{13}$	δ_{CP}	$\sin^2\theta_{23}$	Δm^2_{23} ($\times 10^{-3}$ eV^2)
SK (NH)	1037.5	0.0218	$4.36^{+0.88}_{-1.39}$	$0.44^{+0.05}_{-0.02}$	$2.40^{+0.11}_{-0.12}$
SK (IH)	1040.7	0.0218	$4.54^{+0.88}_{-1.32}$	$0.44^{+0.09}_{-0.03}$	$2.40^{+0.09}_{-0.32}$

Table 3: Summary of the best fit results for atmospheric neutrino analysis of the full SK-I to IV dataset assuming either normal or inverted hierarchy. P-value for this χ^2 is about 0.32.

With the increased precision on the measurement of oscillation parameters, SK is also sensitive to sub-dominant effects and new physics, *e.g.* non-standard neutrino interactions (NSI) which modify the effective Hamiltonian and therefore the oscillation probability. So far, SK data are consistent with no contribution from NSI. Employing atmospheric neutrinos SK can also probe other effects that modify the oscillation probability such as Lorentz invariance violation or additional neutrino states.

2.2 Supernovae physics with Super-Kamiokande

Core-collapse supernovae (CCSNe) are among the most cataclysmic phenomena in the Universe and are essential elements of the dynamics of the cosmos. Their underlying mechanism is however still poorly understood, as characterizing it would require intricate knowledge of the core of the collapsing star. Information about this core could be accessed by detecting neutrinos emitted by supernova bursts, whose luminosity and energy spectra closely track the different steps of the CCSN mechanism. Existing neutrino experiments, however, are mostly sensitive to supernova bursts occurring in our galaxy and its immediate surroundings, that are extremely rare (a few times per century in our galaxy). So far, only SN1987a which occurred on 23 February 1987 in the Large Magellanic Cloud (LMC) has been detected by neutrino experiments: Kamiokande II, IMB and Baksan. Kamiokande II only detected 12 events. With SK, we expect to detect

[1] An unconstrained analysis where $\sin^2\theta_{13}$ is also fitted is also possible but with less sensitivity to other parameters

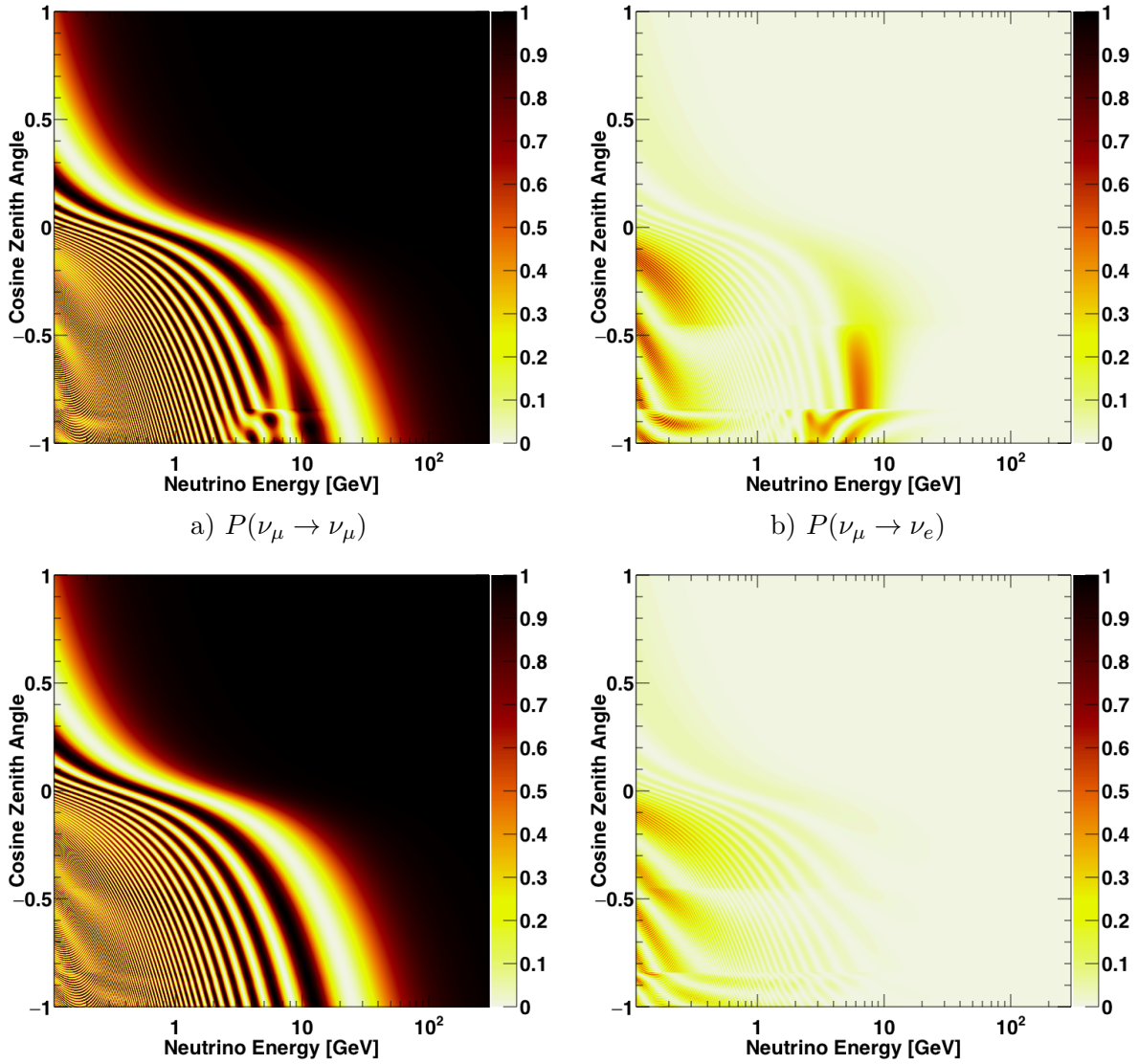

a) $P(\nu_\mu \to \nu_\mu)$ b) $P(\nu_\mu \to \nu_e)$

c) $P(\bar{\nu}_\mu \to \bar{\nu}_\mu)$ d) $P(\bar{\nu}_\mu \to \bar{\nu}_e)$

Figure 3: Oscillation probabilities for neutrinos (upper panels) and antineutrinos (lower panels) as a function of energy and zenith angle assuming a normal mass hierarchy. Matter effects in the Earth produce distortions in the neutrino oscillograms between two and ten GeV, which are not present in the antineutrino oscillograms. Distortions in the ν_μ survival probability and enhancements in the ν_e appearance probability occur primarily in angular regions corresponding to neutrino propagation across both the outer core and mantle regions (cosine zenith < -0.9) and propagation through the mantle and crust ($-0.9 <$ cosine zenith < -0.45). For an inverted hierarchy the matter effects appear in the antineutrino figures instead. Here the oscillation parameters are taken to be $\Delta m^2_{32} = 2.5 \times 10^{-3}$ eV^2, $\sin^2\theta_{23} = 0.5$, $\sin^2\theta_{13} = 0.0219$, and $\delta_{\rm CP} = 0$ [10].

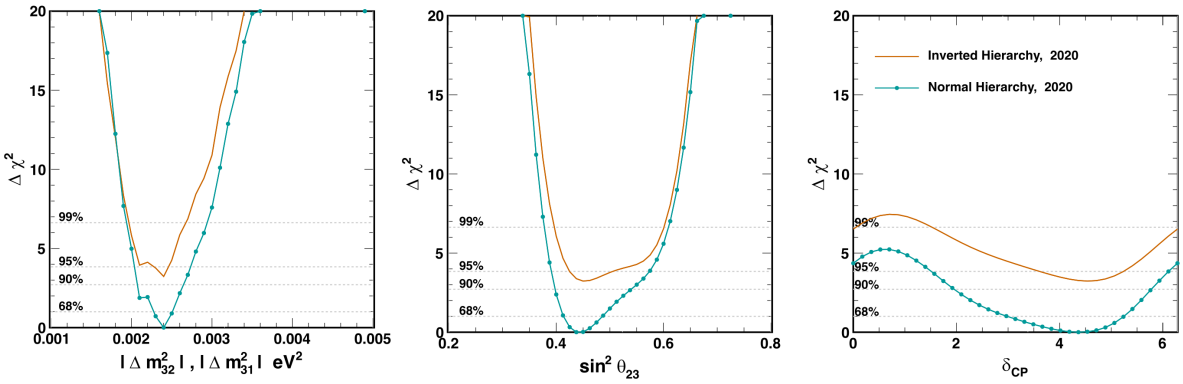

Figure 4: Atmospheric neutrino analysis fit results for full SK-I to IV dataset with constrained θ_{13}. Inverted hierarchy result (orange) is offset from the normal hierarchy result (blue) by the difference in their minimum χ^2.

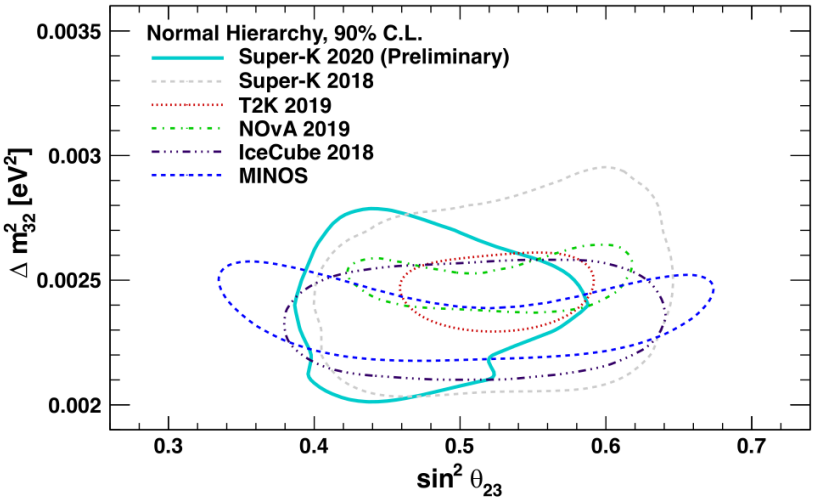

Figure 5: Allowed regions at 90% C.L. in the $(\sin^2\theta_{23}, \Delta m^2_{23})$ plane for SK in the NH compared with other experimental results.

$\sim$ 8000 neutrino events in the ID for a SN in the galactic center, allowing to better constraint the CCSN mechanism. This prospect motivates the collaboration to constantly search for SN bursts with dedicated algorithms.

Learning about SNe properties can also be done by searching for the DSNB. The DNSB is composed of neutrinos of all flavors whose energies have been redshifted when propagating to the Earth. Its spectrum therefore contains unique information not only on the SN neutrino emission process but also on the star formation and Universe expansion history. Spectra predicted from various models are shown in the left panel of Fig. 6. Their normalization is mostly determined by the SN rate, related to the cosmic star formation rate. Their shape depends on many parameters *e.g.* fraction of black-hole-forming SN, effective neutrino energies (related to the core temperature), and sub-dominantly on the expansion of the Universe (through the effect of the red-shift) and the neutrino mass hierarchy for example.

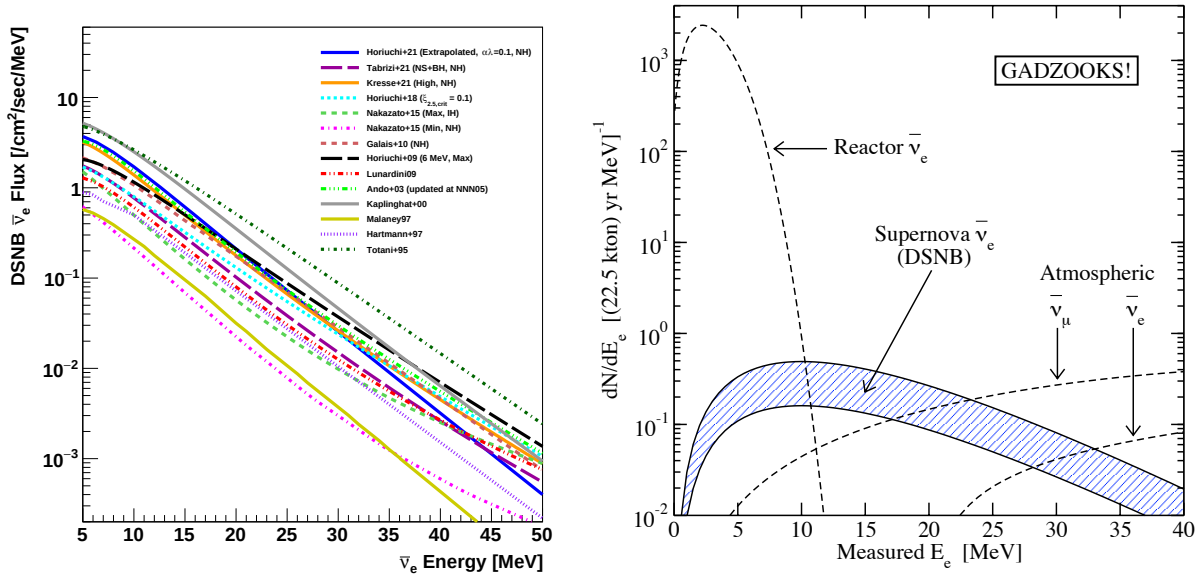

Figure 6: (Left) DSNB $\bar{\nu}_e$ flux predictions from various theoretical models. Taken from [13]. (Right) Expected detection rates in SK through inverse beta decay (IBD) [16].

A significant fraction of DSNB neutrinos are expected to have energies lower than 10 MeV. However, in this energy region, the signal is overwhelmed by reactor antineutrinos, solar neutrinos, muon spallation and natural radioactivity. For energies $\gtrsim$ 30 MeV, the DSNB signal becomes much smaller than atmospheric neutrinos fluxes. It is therefore searched for at energies of $\mathcal{O}(10)$ MeV. At these energies, the detection channel in SK is the inverse beta decay (IBD) $\bar{\nu}_e + p \rightarrow e^+ + n$, its cross section being larger by two orders of magnitude than the second-leading interaction channel. In order to disentangle the signal from various backgrounds, the detection of the neutron in coincidence with the positron is mandatory. The expected detection rate of DSNB through IBD is shown on right panel of Fig. 6. The neutron doesn't produce any Cherenkov scintillation light directly but its capture on a proton leads to the emission of a 2.2 MeV photon with a characteristic timescale of $\sim$ 200 μs. The current neutron detection efficiency is of about 25%.

There are currently two DSNB analyses at SK [13] : the first one is model independent and the second one is a spectral fit to many different models. The model-independent analysis uses the SK-IV dataset and requires one neutron to be tagged[2]. With respect to previous results [14, 15] the reconstructed energy threshold has been lowered from 11.5 to 7.5 MeV thanks to an improved neutron tagging algorithm based on a boosted decision tree (BDT).

[2]before SK-IV and its upgraded electronics the acquisition window was too small to look for delayed neutron capture

The reconstructed neutrino energy spectrum for the full SK-IV data after all selection cuts being applied is displayed on the left panel of Fig. 7. The derived energy dependent limit on the DSNB $\bar{\nu}_e$ flux and its comparison with other experimental results as well as theoretical predictions is displayed on right panel of Fig. 7. The spectral fit analysis consists in deriving the model-dependent limit on the DSNB flux by fitting signal and background spectral shapes to the observed data in the 15.5-79.5 MeV range, and combining the obtained results with the ones from previous SK phases. As in the model-independent analysis a BDT is used to identify delayed neutrons. However events with zero or more than one neutron are not discarded, so as to keep enough signal events in spite of the higher energy threshold. The obtained 90% C.L. upper limits on the DNSB $\bar{\nu}_e$ flux and improvements with respect to previous SK analysis [14] are shown on Fig. 8.

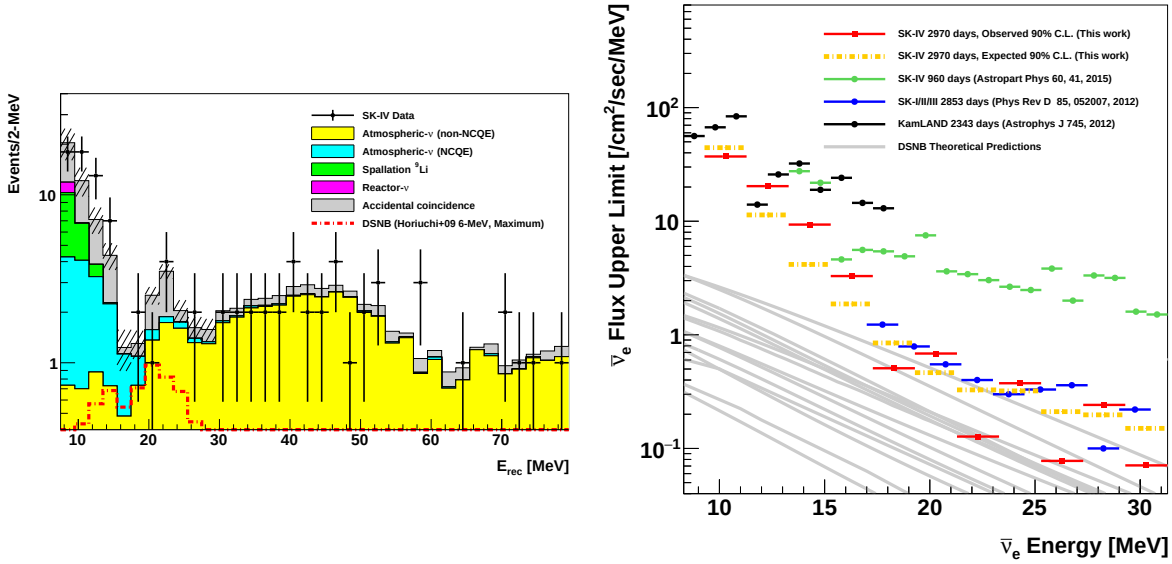

Figure 7: (Left) Reconstructed energy spectrum after data reductions for the background expectation and observation including the signal window and the sideband region. The hatched histogram in the signal window represents the total systematic uncertainty. The red dashed line represents a DNSB signal expectation from the Horiuchi+09 model shown only for the signal window. (Right) 90% C.L. expected and observed limits on the extraterrestrial electron antineutrino flux from the 2021 analysis, in comparison with previously published results from SK and KamLAND, and DSNB theoretical predictions. Both plots are taken from [13].

The LLR team currently has the leadership of the DSNB analyses with the SK-IV dataset. We worked on the simulation of both the DSNB signal and backgrounds and developed the BDT for neutron tagging. These tools are both used in both model-independent and spectral fit analyses. We performed the spectral fit analysis (including the evaluation of all systematics) and combined its results with the observations from SK-I, II, III. We are also working on the modeling of the spallation background (a dedicated paper is currently under collaboration review). This work includes a dedicated modeling of the relevant nuclear processes with FLUKA and the propagation of the obtained results with the official SK simulation code. It has been validated against SK data. All this work will serve for the optimization of the spallation rejection cuts for the future analyses with the new datasets of the SK-Gd phase. Additionally, we are developing a simulation chain to model both DSNB signal and background with modern tools (GEANT4) both for the new SK-Gd phase and for sensitivity studies for Hyper-Kamiokande, as well as an improved reconstruction framework for low energy events.

3 Future of the Super-Kamiokande experiment

In August 2020, the SK collaboration finished adding Gadolinium (Gd) to the 50 ktons of water of its tank. Without any doubt, we are entering an era of extraordinary research with the next generation of this detector, whose flagship program is the search for the DSNB. In SK, many analyses are highly affected by the limited ability to discriminate between neutrinos and antineutrinos, whose charged current interactions produce a hadronic component as well as a charged lepton. SK being non-magnetized, there is no simple way to discriminate between the lepton charges and therefore, the experiment relies on the hadronic information to separate neutrinos and antineutrinos. Below 1 GeV, the hadronic component is either a proton or a neutron for neutrino and antineutrino interactions respectively. However, these particles cannot be easily detected in SK. As a result, most analyses could not separate neutrinos and antineutrinos for years, which highly limited the already excellent sensitivity of the experiment. The addition of Gd has finally allowed to lift all these limitations by discriminating neutrons from protons, and therefore unambiguously differentiate neutrinos from antineutrinos. Indeed, Gd has one of the largest neutron capture cross-sections and yields a rather clean signal made of a cascade of gamma rays with a total energy of 8 MeV.

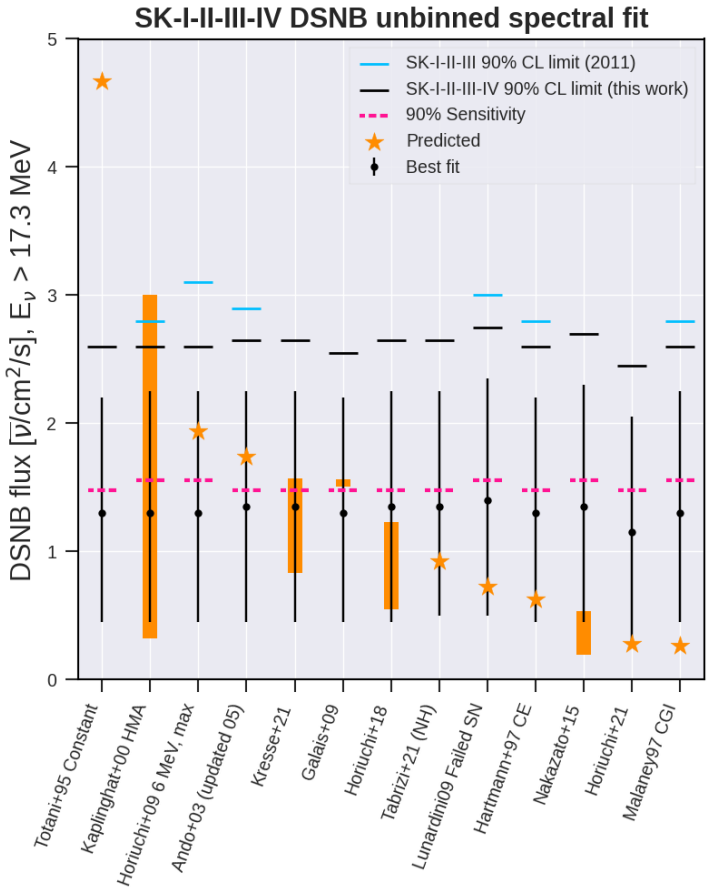

Figure 8: The 90% C.L. upper limits, best-fit values, and expected sensitivities for the DSNB fluxes associated with different models. The best fit fluxes are shown with their associated 1σ error bars. This figure also shows the predictions for each models, either as a range or as one value. Note the stability of the expected and observed flux limits across all models [13].

Before adding Gd to ultrapure water, the SK collaboration validated the concept thanks to a demonstrator called EGADS [17], a 200-ton experiment analogous to a smaller version of SK. The results of EGADS show no decrease in the water transparency of the detector and

established that the Gd dissolving and filling system was working properly. From July 14 to August 17, 2020, 13 tons of Gd have been introduced into the SK tank to reach a concentration of 0.01%, achieving a neutron detection efficiency of about 50%. In September 2020, we started to record the first neutron captures on Gd opening up a new area of discoveries. The schedule is to reach a concentration of 0.03% by 2022 and increase this concentration up to 0.1% to reach a neutron capture efficiency of 90%.

Increasing the neutron tagging efficiency in the DSNB search will increase the statistics by up to a factor ~ 4 assuming a final loading of 0.1% Gd (90% tagging efficiency with respect to the current 25%). The higher energy of the gamma produced after neutron capture on Gd (8 MeV compared to 2.2 MeV on hydrogen) will help lowering the threshold for the analysis by removing almost all of the spallation backgrounds down to 12 MeV, where ^{9}Li background starts to be non-negligible. A work still needs to be undertaken to remove the NC atmospheric background which will become dominant after spallation backgrounds being removed. Some ideas have emerged recently [18] hinting that the NC background could be reduced to 2% of the original rate keeping 96% signal efficiency. If we can get rid of the NC background the 90% C.L. could be comparable to DSNB predictions based on the spectrum of 1987a.

For atmospheric neutrinos oscillations, the gain of having Gd in the tank is twofold. Increasing the neutron capture efficiency allows for a much better separation between neutrinos and antineutrinos and therefore helps determining the mass hierarchy. Neutrons carry part of the initial energy of the neutrino ; however their capture on free protons is almost invisible. Therefore increasing the visibility of neutron capture using Gd helps obtaining a better energy reconstruction relevant for atmospheric neutrino studies. Dedicated sensitivity studies still need to be undertaken.

Concerning the future of the group, we have one clear weakness identified. Two post-docs and one PhD student will leave the group before the end of 2021, shrinking our working force. Moreover, Michel Gonin (DRCE) has left our group to take in charge the head of the IRL ILANCE, International Research Laboratory between France and Japan. We definitely need to reinforce our team in term of new physicists, ideally with one post-doc and one permanent physicist. One PhD student will join the group in October. Concerning the IN2P3 funding, we do not foresee any technical contribution and keeping it at the same level seems fair enough.

References

[1] `https://cordis.europa.eu/project/id/872549`

[2] Y. Fukuda *et al.* [Super-Kamiokande], "The Super-Kamiokande detector", Nucl. Instrum. Meth. A **501** (2003), 418-462

[3] K. Abe *et al.* [Super-Kamiokande], "Calibration of the Super-Kamiokande Detector", Nucl. Instrum. Meth. A **737** (2014), 253-272

[4] K. Abe *et al.* [T2K], "The T2K Experiment", Nucl. Instrum. Meth. A **659** (2011), 106-135

[5] LLR and LNPHE neutrino groups "IN2P3 contributions to T2K", Prepared for the IN2P3 scientific council (October 2021)

[6] M. Honda, T. Kajita, K. Kasahara and S. Midorikawa "Improvement of low energy atmospheric neutrino flux calculation using the JAM nuclear interaction model" Phys. Rev. D **83** (2011), 123001

[7] Y. Hayato, "NEUT," Nucl. Phys. B Proc. Suppl. **112** (2002), 171-176

[8] Y. Fukuda *et al.* [Super-Kamiokande], "Evidence for oscillation of atmospheric neutrinos," Phys. Rev. Lett. **81** (1998), 1562-1567

[9] K. Abe *et al.* [Super-Kamiokande], "Evidence for the Appearance of Atmospheric Tau Neutrinos in Super-Kamiokande," Phys. Rev. Lett. **110** (2013) no.18, 181802

[10] M. Jiang *et al.* [Super-Kamiokande], "Atmospheric Neutrino Oscillation Analysis with Improved Event Reconstruction in Super-Kamiokande IV," PTEP **2019** (2019) no.5, 053F01

[11] P.A. Zyla et al. (Particle Data Group), Prog. Theor. Exp. Phys. 2020, 083C01 (2020) and 2021 update

[12] K. Abe *et al.* [T2K], "Constraint on the matter–antimatter symmetry-violating phase in neutrino oscillations," Nature **580** (2020) no.7803, 339-344 [erratum: Nature **583** (2020) no.7814, E16]

[13] K. Abe *et al.* [Super-Kamiokande], "Diffuse Supernova Neutrino Background Search at Super-Kamiokande," arXiv:2109.11174 [astro-ph.HE].

[14] K. Bays *et al.* [Super-Kamiokande], "Supernova Relic Neutrino Search at Super-Kamiokande," Phys. Rev. D **85** (2012), 052007

[15] H. Zhang *et al.* [Super-Kamiokande], "Supernova Relic Neutrino Search with Neutron Tagging at Super-Kamiokande-IV," Astropart. Phys. **60** (2015), 41-46

[16] J. F. Beacom, "The Diffuse Supernova Neutrino Background," Ann. Rev. Nucl. Part. Sci. **60** (2010), 439-462

[17] L. Marti, M. Ikeda, Y. Kato, Y. Kishimoto, M. Nakahata, Y. Nakajima, Y. Nakano, S. Nakayama, Y. Okajima and A. Orii, *et al.* "Evaluation of gadolinium's action on water Cherenkov detector systems with EGADS," Nucl. Instrum. Meth. A **959** (2020), 163549

[18] D. Maksimović, M. Nieslony and M. Wurm, "CNNs for enhanced background discrimination in DSNB searches in large-scale water-Gd detectors," [arXiv:2104.13426 [physics.ins-det]]